



Received on 07 May 2019; received in revised form, 12 January 2020; accepted, 29 January 2020; published 01 March 2020

XANTHAN GUM GRAFT COPOLYMER / SODIUM ALGINATE MICRO BEADS COATED WITH CHITOSAN FOR CONTROLLED RELEASE OF CHLORTHALIDONE DRUG

T. Jithendra ¹, O. Sreekanth Reddy ¹, M. C. S. Subha ^{*1}, C. Madhavi ² and K. Chowdoji Rao ²

Department of Chemistry ¹, Department of Polymer Science and Technology ², Sri Krishnadevaraya University, Ananthapuramu - 515003, Andhra Pradesh, India.

Keywords:

Sodium alginate, Xanthan gum grafted N, N'-methylene diacrylamide, Chitosan, Microbeads, Drug delivery

Correspondence to Author:

Prof. M. C. S. Subha

UGC-BSR Faculty Fellow,
Department of Chemistry,
Sri Krishnadevaraya University,
Ananthapuramu - 515003, Andhra Pradesh, India.

E-mail: mcsubha3@gmail.com

ABSTRACT: In the present work, temperature/pH-sensitive copolymer beads of chitosan (CS) coated sodium alginate/xanthan gum grafted N, N'-methylene diacrylamide have been synthesized by free radical polymerization in an atmosphere of nitrogen using AIBN/Fe²⁺ redox pair initiator and Tetramethylethylenediamine (TEMED) as a catalyst followed by simple ionotropic gelation technique. These beads were characterized by Fourier transform infrared (FTIR) spectroscopy, Differential scanning calorimetry (DSC), Field emission scanning electron microscopy (FESEM) Energy-dispersive X-ray spectra (EDS) and X-ray diffraction measurements (X-RD). DSC and X-RD studies reveal the molecular dispersion of Chlorthalidone (CT) drugs. Swelling and drug release behaviors of these beads were investigated in simulated intestinal fluid (pH 7.4) and gastric fluid (pH 2.0) at 37 °C. Results illustrated that both the swelling and degradation of the optimized beads were influenced by the pH of the test medium, which might be suitable for intestinal drug delivery. The release mechanism was analyzed by fitting the release data into the Korsmeyer-Peppas equation.

INTRODUCTION: Hydrogels are a hydrophilic three-dimensional network of polymer chains formed from homopolymers, copolymers or macromers. Hydrogels are highly absorbent natural or synthetic polymeric networks, sometimes found as a colloidal gel in which water is the dispersion media. Hydrogels also possess a degree of flexibility very similar to natural tissue, due to their significant water content ¹. Hydrogels are environmentally sensitive to small changes in environmental parameters such as temperature, pH, or the concentration of metabolite and release their load as a result of such a change ².

Temperature-/pH-sensitive hydrogels are widely used in a variety of biomedical or pharmaceutical applications, such as molecular separation ³, tissue engineering ⁴ and particularly in fabricating the controlled drug delivery systems ⁵.

Chlorthalidone CT **Fig. 1** [2-chloro-5-(1-hydroxyl-3-oxo-2, 3-dihydro-1H-indol-1-yl) benzene-1-sulfonamide] tautomerizes to a benzophenones form ⁶. CT is an antihypertensive thiazide-like diuretic used in the treatment of edema associated with congestive heart failure. Compared with other thiazides like chlorothiazide, CT also shows long-lasting diuretic action. It is absorbed slowly from the gastrointestinal tract and is excreted largely as an unchanged drug. The overall duration of effect is 48 to 72 h and its usage in drug delivery application is scanty ⁷. Xanthan gum (XG) is a heteropolysaccharide consisting of β-D-glucose, α-D-mannose and α-D-glucuronic acid ⁸. Due to the presence of glucuronic acid and pyruvic acids in

QUICK RESPONSE CODE 	DOI: 10.13040/IJPSR.0975-8232.11(3).1132-45
	The article can be accessed online on www.ijpsr.com
DOI link: http://dx.doi.org/10.13040/IJPSR.0975-8232.11(3).1132-45	

the side chain of XG, it shows anionic nature. XG has good drug retarding ability, prevent initial burst release, inertness and biocompatibility, due to these properties XG can be used as a drug carrier in drug delivery systems⁹⁻¹¹.

Sodium alginate (SA) is natural, an anionic linear polysaccharide when it combines with water it forms a gluey gum. This biopolymer is made up of linear unbranched copolymers that contain alternating blocks of (1-4)-linked β -D-mannuronic acid (M) and (1-4)-linked α -L-glucuronic acid (G) residues¹². Alginates are considered biocompatible, biodegradable, chemical versatility and non-toxicity for medical applications. Alginates have attracted much attention as carriers for drug and cell delivery¹³. Na^+ ions of glucuronic acid residues interact ionically with multivalent cations (usually Ca^{2+}) and then the α -L-glucuronic acid groups can connect with each other, resulting in a three-dimensional hydrogel network which has pH-sensitive property¹⁴. Generally, hydrogels suffer from some serious problems, such as hydrogels are hydrated and porous like living tissues¹⁵ and also brittle in nature¹⁶, which have poor mechanical strength. Drug encapsulation efficiency decreases due to larger pores that may result in leakage of an entrapped drug into the external medium¹⁷. Burst release of the drug from the natural hydrogels is due to the breakdown of beads *in-vitro* conditions¹⁸. In order to solve these problems currently much effort has been spent on improving the gel beads. Previously Talukdar *et al.*,^{19, 20} have reported that XG has important pharmaceutical and economical advantages *i.e.* less susceptible to erosion during drug release, higher drug retarding ability, absence of initial burst release. Rajat *et al.*,²¹ reported that XG shows a sustainable drug release pattern to reduce dosing frequency. Yongzhen *et al.*,²² suggested that

chemical crosslinking XG-STMP hydrogels show the stronger elastic property, tough to resist deformation, good swelling and sustained drug release properties than the physical hydrogel.

Gomez *et al.*,²³ suggested that ionotropically cross-linked alginate hydrogels have low stability and initially lose their mechanical stability as time passes. Fareez *et al.*,²⁴ reported that the inclusion of three polymers (XG, SA and CS) shows good miscibility for microencapsulation due to molecular interaction of XG and SA, which led to the formation of a matrix structure. Thaned *et al.*,²⁵ suggested that XG could modulate physicochemical properties and drug release of the gel beads, which is based on the existence of molecular interaction of XG and SA. Previously huge work was carried out using hydrophobic type of monomers such as ethyl acrylate²⁶, acrylamide²⁷, acrylic acid²⁸ and vinyl pyrrolidone²⁹. To improve water absorbency and hydrophilic nature, the monomers must contain hydrophilic nature, for this reason, we have chosen N, N'-methylene-diacrylamide (MDA) grafted XG. Previously grafting of MDA on to cellulose and silk fibers has been reported^{30,31}.

In the present study the graft copolymer has been blended with SA to prepare temperature-/pH-responsive CXG-g-MSB, which are coated with chitosan (CS) to form a shell on gel beads to improve their mechanical strength, encapsulation efficiency and their stability on swelling and drug release behaviors. This improvement is achieved by coating the hydrogels formed from the graft copolymer of XG and SA with CS. A schematic diagram of the present work is shown in **Fig. 2**. The effect of CS coated shell on swelling behavior and drug release studies are estimated.

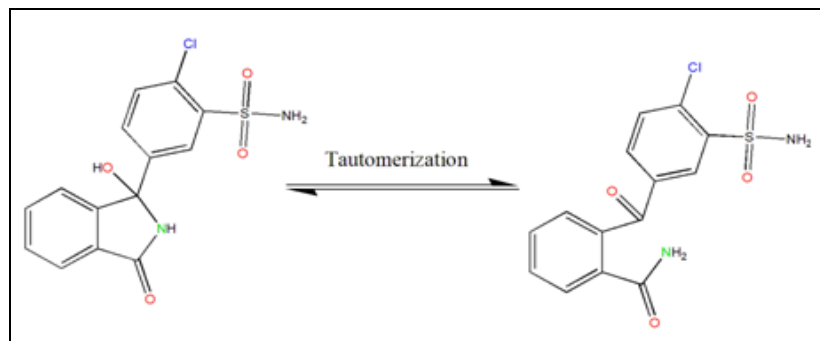


FIG. 1: STRUCTURE AND TAUTOMERIZATION OF CT

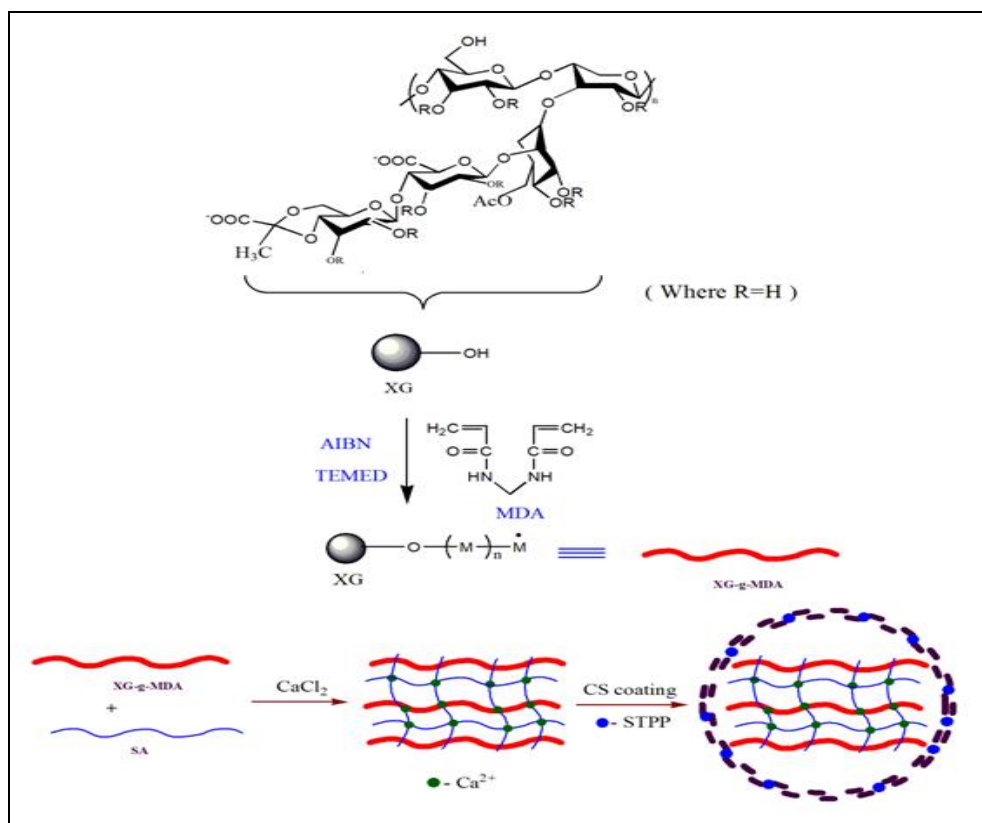


FIG. 2: SCHEMATIC REPRESENTATION OF THE FORMATION OF CS COATED MICRO BEADS

EXPERIMENTAL:

Materials: Sodium alginate, xanthan gum, chitosan, tetramethylethylenediamine (TEMED) and azobisisobutyronitrile (AIBN) were purchased from Sigma–Aldrich (USA). Sulfuric acid was purchased from M/S moly chemicals, Mumbai (India). N, N'-methylene diacrylamide (MDA), sodium triphosphate penta basic (STPP), ferrous sulphate and calcium chloride (CaCl_2) were purchased from Sd. Fine chemicals, Mumbai, India. Chlorthalidone gift sample was obtained from M/S Suven Life Sciences Ltd. Hyderabad. Water used was of high purity grade after double distillation.

Synthesis of N, N'-methylene diacrylamide-grafted- Xanthan Gum (XG-g-MDA): The graft copolymerization of MDA onto XG has been carried out in a 250 mL round bottom flask. The flask was placed on a water bath which is fitted with an electrically operated magnetic stirrer (Remi Motors, India), maintained at temperature 70 ± 2 °C. A solution of XG (0.125 gm in 25 mL of water) placed in 250 mL round bottom flask with constant stirring and nitrogen gas is passed as a stream for about 15 min desired quantity of MDA, sulfuric acid and ferrous sulfate solutions were mixed with the XG solution²⁸.

Afterwards, oxygen-free nitrogen gas was purged through the solution mixture for 30 min. At this stage, AIBN as initiator and TEMED as catalyst was added and nitrogen gas purging were continued for another 2 h, after which it was terminated by adding a saturated solution of hydroquinone.

The reaction mixture was cooled to room temperature and this was poured into an excess amount of acetone, taken in a 500 mL beaker, to remove the unreacted monomer. Thus graft material was precipitated, dried under vacuum at a constant weight.

The grafting percentage (G%), efficiency percentage (E%), conversion percentage (C%), and homopolymer percentage (HP%) were calculated see **Table 1** using Equations. (1) – (4) respectively.

$$\text{Grafting percentage (G\%)} = (W_2 - W_0) / W_0 \times 100 \dots \dots \dots (1)$$

$$\text{Efficiency percentage (E\%)} = (W_2 - W_0) / (W_1 - W_0) \times 100 \dots \dots \dots (2)$$

$$\text{Conversion percentage (C\%)} = (W_1 - W_0) / W_3 \times 100 \dots \dots \dots (3)$$

$$\text{Homo-Polymer Percentage (HP\%)} = 100 - E\% \dots \dots \dots (4)$$

Where W_0 is the weight of XG in grams; W_1 is weight of the XG-g-MDA in grams before washing; W_2 is the weight of XG-g-MDA in grams

after washing and W_3 is the weight of MDA used in grams.

TABLE 1: THE CALCULATED VALUES FOR % GRAFTING (%G), % EFFICIENCY (%E), % CONVERSION (%C) AND % HOMO POLYMER (% HP)

S. no.	Sample	G %	E %	C %	HP %
1	XG-g-MDA	32.6	80.02	67.90	19.98

Preparation Procedure of CT Loaded Blend Beads: CT-loaded XG-g-MSBs and CS coated CXG-g-MSBs were prepared by the following procedures. Briefly, XG-g-MDA and SA aqueous dispersions 2% (w/v) of each were prepared separately using distilled water. Different XG-g-MDA/SA blends were prepared by mixing 60:40 (XG-g-MSB-a) and 80:20 (XG-g-MSB-b). These solutions of XG-g-MSB blends were well mixed (as per the formulations given in **Table 2** with stirring for 2 h at 400 rpm using a magnetic stirrer (Remi Motors, India). Afterward, sodium triphosphate penta basic and CT was added into the XG-g-MSB solution, placed in a sonicator for 10 min and dispersed homogeneously using a magnetic stirrer. The above-mixed solution was transferred dropwise into the CaCl_2 solution, the

spherical beads formed instantly were kept for 40 min. The above formulations (XG-g-MSB-a and XG-g-MSB-b) are coated with CS using the following procedure. The above formulations are mixed well by the same procedure as discussed above, the mixed solution was transferred dropwise into the mixed solution containing CaCl_2 and CS under gentle stirring, the spherical beads formed instantly were kept for 40 min. The CS concentration was 0.4% and 0.6%, the corresponding samples were accordingly named as CXG-g-MSB-4a, CXG-g-MSB-4b and CXG-g-MSB-6a, CXG-g-MSB-6b, respectively see **Table 2**. The wet beads obtained collected by decantation, washed three times with distilled water to remove the drug attached on the bead surface, and finally were dried in air overnight and then vacuum-dried to constant weight at 40 °C.

TABLE 2: COMPOSITIONS AND ENCAPSULATION EFFICIENCY (% EE) OF ALL SAMPLES

S. no.	Sample	XG-g-MDA (%)	SA (%)	CS (Wt %)	Drug (mg)	% EE
1	XG-g-MSB-a	60	40	0.0	40	51.31
2	XG-g-MSB-b	80	20	0.0	30	49.56
3	CXG-g-MSB-4a	60	40	0.4	40	56.14
4	CXG-g-MSB-4b	80	20	0.4	30	61.40
5	CXG-g-MSB-6a	60	40	0.6	40	59.71
6	CXG-g-MSB-6b	80	20	0.6	30	63.74
7	XG-g-MSB	80	20	0.0	00	00.00

Characterizations Methods:

Fourier Transform Infrared (FTIR) Spectral Analysis: FTIR (Bomem MB-3000 Make: Canada) with Horizon MBTM FTIR software was used to record the spectrum of grafted, non-grafted and drug-loaded samples to find out the possible chemical interactions between polymer, monomer and drug.

The finely powdered and dried samples were mixed by crushing 5 mg of the polymer with 100 mg of KBr in a pestle and mortar. Pellets were prepared under a hydraulic pressure of 600 kg/cm². These pellets were again crushed and repelled. This step was repeated 2-3 times to get better reproducibility. Spectra were taken in the wavelength range 400-4000 cm⁻¹.

Differential Scanning Calorimetry (DSC):

Differential scanning calorimetry scans were measured to explore the thermal behavior of pure drug, drug-loaded microbeads and placebo microbeads. The scans were recorded on a differential scanning calorimeter between 30 °C to 300 °C at a heating rate of 10 °C/min under nitrogen atmosphere.

X-Ray Diffraction (X-RD) Analysis:

The X-ray diffraction of the plain gel beads, drug-loaded gel beads and CS coated gel beads were performed by a wide-angle X-ray scattering diffractometer (Panalytical X-ray Diffractometer, model-X'pert Pro) with $\text{CuK}\alpha$ radiation ($\lambda = 1.54060$) at a scanning rate of 5 °C/min to determine the crystallinity.

Field Emission Scanning Electron Microscopy (FESEM) Analysis: The morphological characterization of the gel beads was observed using FESEM (Make: JEOL, Singapore. Model: JEOL JSM-7100F) with an accelerating voltage of 20 kV equipped with an EDS detector.

Swelling Measurements: The swelling degrees of CXG-g-MSB and XG-g-MSB's of different formulations were determined gravimetrically. The dried beads (50 mg) were weighed accurately and soaked into 30 mL of pH 7.4 phosphate buffer solution at 37 °C. At predetermined time intervals *i.e.*, 1, 2, 3, 4, 5, 6, 7, 8 h the swollen beads were taken out and placed on dry filter paper to absorb the excess water and then the beads were weighed on an electronic microbalance (Adam, AAA 160 L, U.K.; accuracy 0.0001 g). This process is continued until the weight of swollen beads reached a constant value. The swelling degree (SD_t) was calculated using the following equation:

$$\text{Swelling degree (SD)}_t = (W_s - W_d) / W_d \times 100 \dots \dots \dots (5)$$

Where W_s is the weight of swollen beads and W_d is the weight of dry beads.

In-vitro Drug Release:

Determination of Encapsulation Efficiency: Percentage of encapsulation efficiency was estimated according to the formula and method reported in previous literature³². A known mass of beads (10 mg) was immersed into 100 mL of phosphate buffer solution (pH 7.4 containing 5% absolute ethyl alcohol) for 24 h and then the beads were crushed to ensure the complete extraction of CT from the beads. The absorbance of the clear supernatant buffer solution containing the extracted amount of CT was measured by UV-Vis spectrophotometer (Lab India, Mumbai, India) at the λ_{max} value of 274 nm for CT with pH 7.4 buffer solution as a blank. The concentration of drugs was determined by using a calibration curve constructed by a series of CT standard solutions. The percentage of encapsulation efficiency was calculated using the following equations.

$$\text{Drug loading (\%)} = (\text{Weight of drug in nanoparticles}) / (\text{weight of nanoparticles}) \times 100 \dots \dots \dots (6)$$

$$\text{EE (\%)} = (\text{Actual drug loading}) / (\text{Theoretical drug loading}) \times 100 \dots \dots \dots (7)$$

In-vitro Drug Release Studies: Study of *in-vitro* drug release kinetics for different formulations was performed at 37 °C using a dissolution tester (Lab India, Mumbai, India) containing eight baskets. Accurate quantity of dried beads (100 mg) was immersed into 900 mL of phosphate buffer solution (PBS) pH 7.4 and pH 2.0 at a rotation speed of 50 rpm to replicate intestinal and gastric fluid atmosphere respectively. At a predetermined time intervals 5 mL of sample was withdrawn and 5 mL of fresh PBS was added back to the basket to keep total volume constant throughout the experiment. The amount of CT released was assayed using a UV-Vis spectrophotometer at 274 nm, and the released drug amount was obtained by using concentration versus absorbance calibration curve.

Drug Release Kinetic Models: The drug release kinetics of zeroth order, first order, Higuchi and Korsmeyer-Peppas models were analyzed by fitting the data on the basis of goodness.

Zeroth Order: Zero-order describes the system where the release rate of the drug is independent of its concentration. To study the drug release kinetics data obtained from the *in-vitro* dissolution study is plotted against time *i.e.*, cumulative drug release *vs.* time^{33,34}.

$$C = k_0 t \dots \dots \dots (8)$$

Where k_0 is zeroth-order rate constant, expressed in units of concentration/time, and t is the duration.

First Order Kinetics: The first order describes the system where the release rate of the drug is dependent on its concentration. Hence, the plot of log cumulative percentage drug remaining versus time, which yields a straight line with slope = $-K/2.303$. First-order drug release kinetics can be expressed by the equation:

$$d_c/d_t = -KC \dots \dots \dots (9)$$

Equation (9) can be expressed as

$$\log C = \log C_0 - K_t/2.303 \dots \dots \dots (10)$$

Where C_0 is the initial concentration of a drug, k is the first-order rate constant and t is the time. First-order kinetics describes the drug dissolution in pharmaceutical dosage forms, such as those containing water-soluble drugs in porous matrices³⁵.

Higuchi Model: Higuchi has proposed a model to describe the drug release from polymer matrices (semi-solid and solid matrices). Higuchi proposed a mathematical equation to describe drug release from the matrix system is given by ³⁶:

$$f_t = KHt^{1/2} \dots \dots \dots (11)$$

Where KH is the Higuchi dissolution constant.

The data obtained were plotted as cumulative percentage drug release versus square root of time, exhibiting linear relationship. Higuchi describes drug release as a diffusion process based on Fick's first law. Higuchi model describes the drug dissolution in pharmaceutical dosage forms like some transdermal system and matrix tablets with water-soluble drugs.

Korsmeyer-Peppas Model: Drug release kinetics is analyzed by plotting the cumulative release data

versus time by fitting to the following empirical equation ³⁷:

$$M_t/M_\alpha = kt^n \dots \dots \dots (12)$$

Where M_t and M_α are the cumulative amount of CT released at time t and equilibrium time, respectively, k is a kinetic constant relating to the hydrogel system, and n is the diffusional exponent which suggests the nature of the release mechanism. The n values are determined from the slope of the plot of $\ln(M_t/M_\alpha)$ versus $\ln t$. A value of $n = 0.5$ indicates the Fickian diffusion (case I transport), while polymer chain relaxation becomes the rate-controlling factor for case II transport (relaxation controlled) if $n = 1.0$. When the value of n is between 0.5 and 1.0, the release follows anomalous or non-Fickian diffusion, where the system will be diffusion and relaxation controlled.

RESULTS AND DISCUSSION:

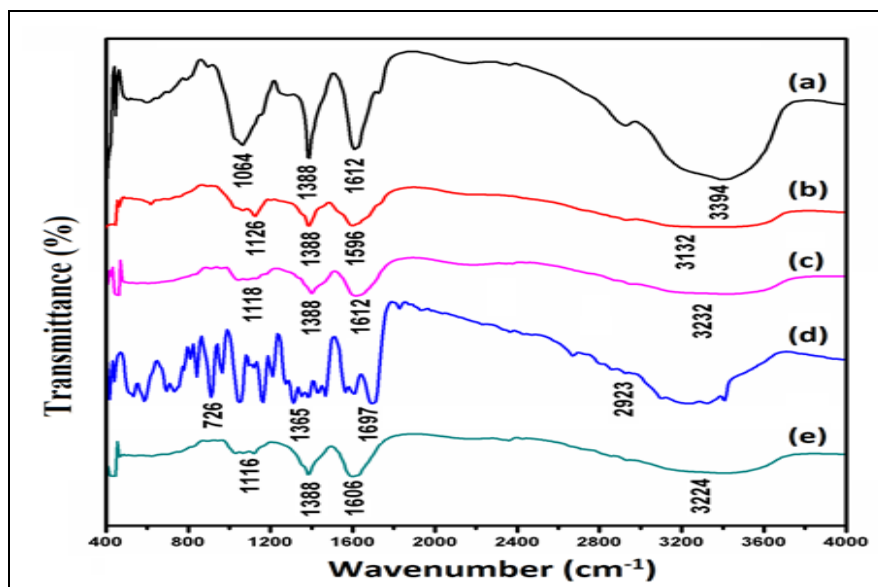


FIG. 3: FTIR SPECTRA OF PURE XG (A), XG-G-MDA (B), PLACEBO MICRO BEADS (C), PRISTINE CT (D) AND CT LOADED MICRO BEADS (E)

FTIR: FTIR spectra of pure XG (a), XG-g-MDA (b), placebo microbeads (c), pristine CT (d) and CT loaded microbeads (e) were illustrated in **Fig. 3**. XG (a) showed broadband at 3394 cm^{-1} corresponding to stretching vibration of hydroxyl (-OH) groups, while, another one appeared at 2983 cm^{-1} corresponding to stretching band of aliphatic hydrocarbon (C-H) groups. Furthermore, the absorption band at 1612 cm^{-1} assigned for stretching carbonyl (-C=O) groups of pyruvate and

absorption band at 1388 cm^{-1} is related to stretching symmetric carboxylate (-COO-) groups of glucuronic acids ³⁸. The FTIR spectra of pristine CT (d) shows a broad peak at $3160\text{-}3485 \text{ cm}^{-1}$ which corresponds to -O-H and -NH₂ groups, band at 2923 cm^{-1} corresponds to C-H stretching frequency, band at 1697 cm^{-1} is assigned for -C=O stretching frequency, bands at 1365 cm^{-1} assigned for aromatic -C=C bending frequency, band at 726 cm^{-1} corresponds to aromatic -C-H bending

frequency. On comparing the FTIR spectra of XG (a) and XG-g-MDA (b), it is observed that O–H stretching frequency peak is decreased in case of XG-g-MDA, indicating the participation of hydroxyl groups of XG with monomers due to chemical reaction, similar observations were reported by Pandey *et al.*,²⁶ from the graft copolymerization of ethyl acrylate onto XG, using potassium peroxydisulfate as an initiator. The graft copolymerization is further confirmed by the characteristic absorption band at 1126 cm^{-1} due to C–O–C stretching frequency in Xg-g-MDA (b).

On comparing the FTIR spectra of placebo microbeads (c) and CT loaded microbeads (e), the C=O stretching frequency shifted from 1612 cm^{-1} to 1606 cm^{-1} in CT loaded microspheres due to the formation hydrogen bonding interaction between a

drug molecule and polymer chains (C=O group and NH group of drug molecule). This indicates the loading of the drug in the microbeads. The appearance of additional peaks in the spectrum of graft copolymer and decreasing of O–H stretching vibration peak in the spectrum of XG-g-MDA showed that grafting might have taken place on OH sites of XG.

Differential Scanning Calorimetry: DSC thermograms of pristine CT (a), placebo microbeads (b), and drug-loaded microbeads (c) are shown in Fig. 4. The pure CT shows a sharp peak at $214.00\text{ }^{\circ}\text{C}$, which corresponds to its polymorphism and melting point respectively. However, these peaks are not observed in drug-loaded microbeads, which confirms the amorphous dispersion of drug molecules in the polymer matrix.

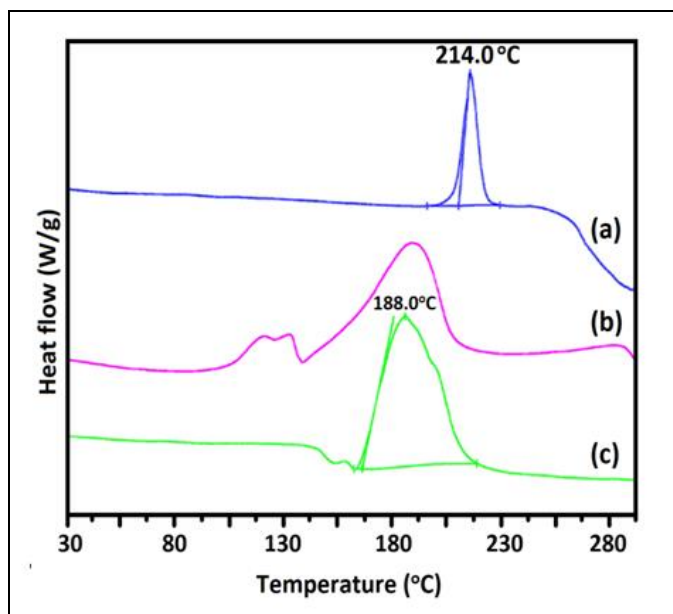


FIG. 4: DSC THERMOGRAMS OF PRISTINE CT (A), PLACEBO MICRO BEADS (B), AND DRUG LOADED MICRO BEADS (C)

X-Ray Diffraction (X-RD) Analysis: X-ray diffractograms of pristine CT (a), CT loaded microbeads (b) and placebo microbeads (c) are displayed in Fig. 5. The most intensive peaks of CT are observed at 2θ of 16.2° , 19.2° and 25.5° representing the crystalline nature of the CT, but these peaks are not observed in CT loaded microbeads, indicating that the drug is dispersed at a molecular level in the polymer matrix. A similar observation was reported by Rao *et al.*,³⁹ from the development of pectin-poly (vinyl pyrrolidone) blend microbeads for controlled release of 5-FU.

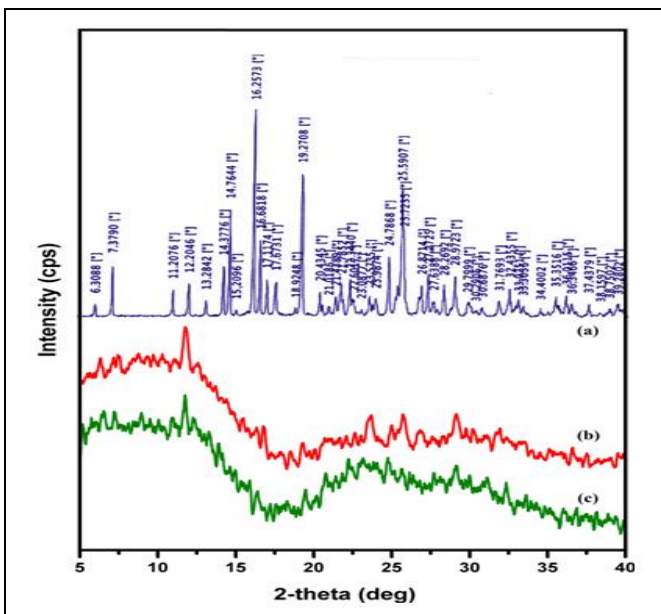


FIG. 5: X-RD PATTERNS OF PRISTINE CT (A), CT LOADED MICRO BEADS (B), AND PLACEBO MICRO BEADS (C)

FESEM and EDS Analysis: The topographical images of XG-g-MSB, XG-g-MSB-a, and CXG-g-MSB-4a was observed using FESEM and are displayed in Fig. 6. From Fig. 6A, B, C it was clear that a thin shell was coated on the surface of CXG-g-MSB-4a but not on XG-g-MSB-a and XG-g-MSB. This gives proof that CS is coated on hydrogel beads. The surface of XG-g-MSB Fig. 6D and XG-g-MSB-a Fig. 6E beads were found to be rough, whereas in CXG-g-MSB-4a Fig. 6F the surface is smooth. It was clear that the coated beads have a smooth surface, which confirms that CS has

been successfully coated on the surface of microbeads. The size of the CS coated beads **Fig. 6F** lies between 1200-1350 μm , whereas the size of uncoated beads **Fig. 6D** and **C** lie between 893-1190 μm . Due to the presence of the CS layer on microbeads the size of the beads increase. This further confirms that CS is coated on the surface of microbeads.

The chemical compositions of the placebo microbeads (XG-g-MSB), drug-loaded microbeads (XG-g-MSB-a) and CS coated microbeads (CXG-g-MSB-4a) were confirmed by energy-dispersive X-ray spectra (EDS) **Fig. 6**. The dominant oxygen peaks in EDS of different microbeads indicate the

presence of hydroxyl groups of the polymer molecules ⁴⁰. In EDS spectra of XG-g-MSB-a, sulphur and nitrogen peaks were observed indicating the presence of the drug in the microbeads whereas in XG-g-MSB these peaks were not observed which indicates that the drug is not loaded in placebo microbeads. But in CXG-g-MSB-4a along with sulphur peaks, nitrogen and phosphorous peaks were observed indicating the presence of STPP and CS, because the STPP contains phosphorous atoms whereas CS contains nitrogen atoms. This confirms that phosphorous interacts with the CS gel shell as a crosslinking agent on the microbeads surface.

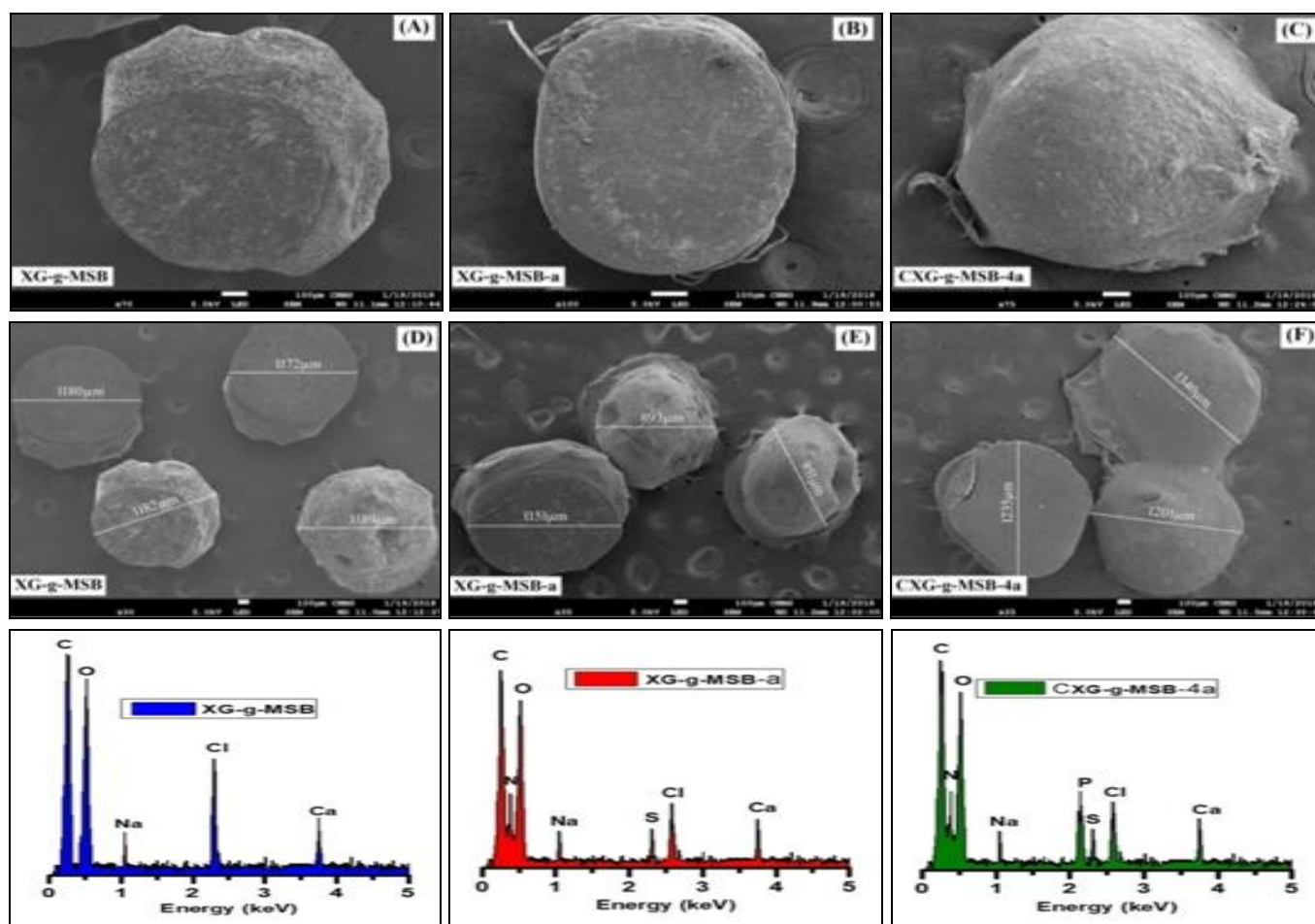


FIG. 6: SCANNING ELECTRONIC MICROSCOPIC IMAGES OF XG-G-MSB (A & D), XG-G-MSB-A (B & E) & CXG-G-MSB-4A (C & F), EDS ANALYSIS OF XG-G-MSB, XG-G-MSB-A & CXG-G-MSB-4A

Swelling Studies: The swelling degree of various formulations are shown in **Fig. 7A** and **7B**. Once the gel beads were placed in a phosphate buffer solution of pH 7.4, the gel beads get partially ionized, and the electrostatic repulsion between COO^- groups takes place, leading to swelling of the polymer. As the grafting content increases, the

swelling ratio of gel beads increase due to its hydrophilicity nature of MDA. The SDt of CXG-g-MSB-6b is higher than the other formulations due to more percentage of CS being a coating in CXG-g-MSB-6b than the other formulations. CS coated on the gel bead surface could absorb water, swell and has more SDt than the uncoated beads.

Sun et al.,¹⁸ also observed the same from the CS coated alginate/poly(N-isopropylacrylamide) beads for dual responsive drug delivery.

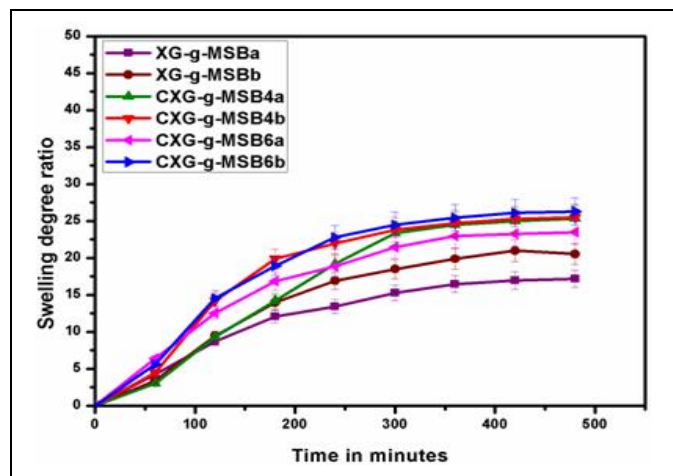


FIG. 7A: SWELLING DEGREE OF ALL THE BEADS UNDER STUDIED IN PH 7.4 AT 37 °C

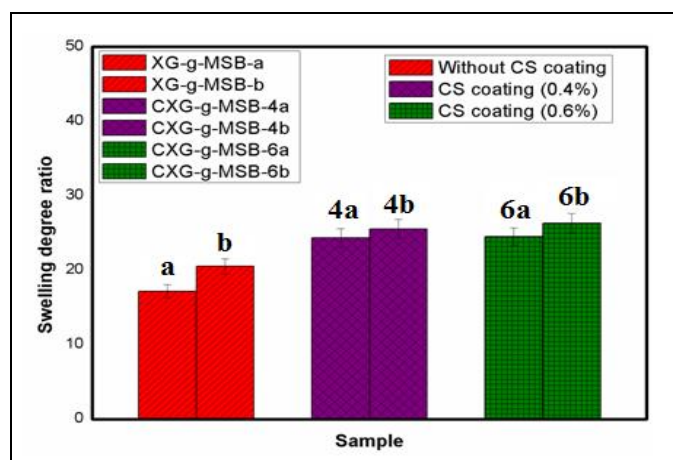
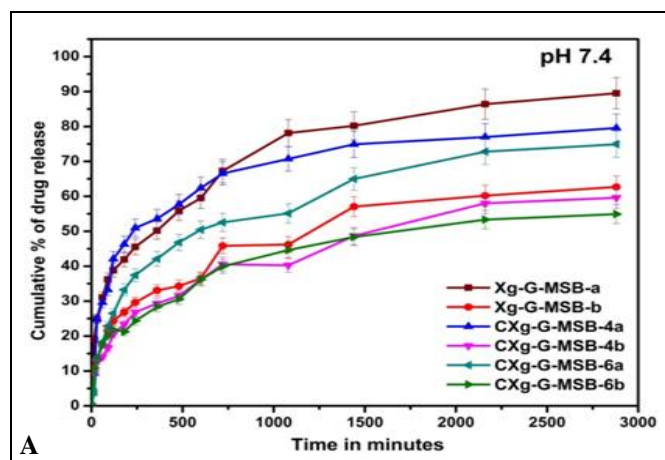


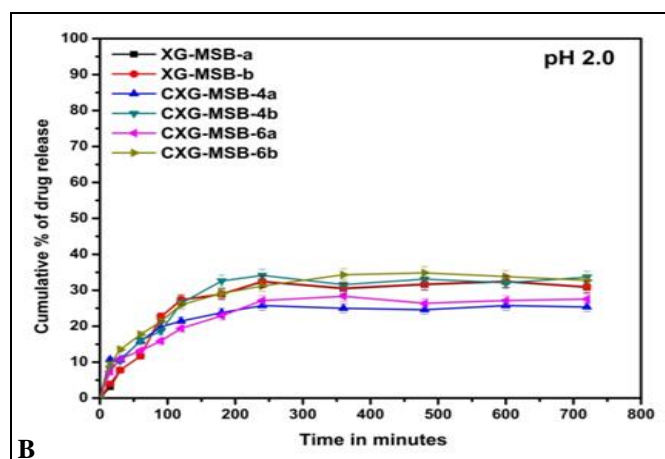
FIG. 7B: COMPARISON OF SWELLING BEHAVIOUR OF HYDROGEL BEADS OF ALL SAMPLES WITH AND WITHOUT COATING OF CS

Encapsulation Efficiency: The percentages of encapsulation efficiency (% EE) of CT loaded microspheres are listed in Table 2, and the value lies in between 49.56% to 63.74%, percentage of EE decreased due to insolubility of CT in water. This indicates the % EE dependence on formulation parameters which include % of blend composition, the extent of drug loading and concentration of CS shell. With an increase in the percentage of SA in the blend matrix, the % EE decreased, because SA might have assisted the diffusion of drug particles into the external surface, to form pores in the matrix. This effect was observed in the formulations of XG-g-MSB-a and XG-g-MSB-b. As the CS coating concentration increases, % EE increased because the presence of

CS shell on the beads diminished the pore sizes, which reduces the leaching out of drug particles to the outer surface during the beads preparation. So, eventually, more amount of drug retains in the microbeads and ultimately increasing the % EE. This effect was observed in the formulations of CXG-g-MSB-4a and CXG-g-MSB-6a, CXG-g-MSB-4b and CXG-g-MSB-6b.



A



B

FIG. 8: CUMULATIVE % OF DRUG RELEASE IN PBS AT (A) PH 7.4 AND (B) PH 2.0 AT 37 °C

In-vitro Drug Release Studies: The cumulative percentage of drug release studies of all profiles is carried out at pH 7.4 and pH 2.0 at 37 °C. *In-vitro* drug release studies are discussed in terms of the effect of pH and effect of CS shell.

Effect of pH: To find out the pH-responsive behavior of microbeads, the *in-vitro* release studies were conducted in both intestinal (7.4) Fig. 8A and gastric (1.2) Fig. 8.B pH environments. From Fig. 8A and 8B, it was clear that the cumulative % of drug release at pH 7.4 was much higher than the pH 2.0. From these results, intestinal fluid (pH 7.4) might be suitable for drug delivery than the gastric

fluid (pH 2.0). In a gastric fluid, the gel beads could bypass without liberating the drug when it is taken as an oral drug carrier. Whereas in intestinal fluid the release rate is higher which is due to the carboxylate groups of SA having fewer interactions with buffer medium at pH 7.4, making the network more slackly, therefore the external medium could diffuse into the microbeads, the drug easily dissolves and leaches out more easily because of the osmotic pressure. A similar observation was reported by Rao⁴¹ from the synthesis of dual responsive carbohydrate polymer-based IPN microbeads for the controlled release of an anti-HIV drug.

Effect of Chitosan Shell: The drug release profiles of XG-g-MSB-a, CXG-g-MSB-4a, and CXG-g-MSB-6a in phosphate buffer solution of pH 7.4 at 37 °C are displayed in Fig. 9. The amount of the drug released was about 89.5%, 79.5%, and 75.0% for XG-g-MSB-a, CXG-g-MSB-4a and CXG-g-MSB-6a respectively. From Fig. 8 it was clear that the cumulative percentage of drug release decreases with an increase in the concentration of CS shell on gel beads.

The decrease of release rate is due to the addition of biomaterialized STPP and CS shell in microbeads. The presence of inorganic STPP holds back the PBS to penetrate into the microbeads at the same time lowers the mechanical stability but the presence of the CS shell improves the mechanical stability of the beads. A similar result was reported by Sun *et al.*,¹⁸ from the chitosan-coated alginate/poly(N-isopropylacrylamide) beads for dual responsive drug delivery.

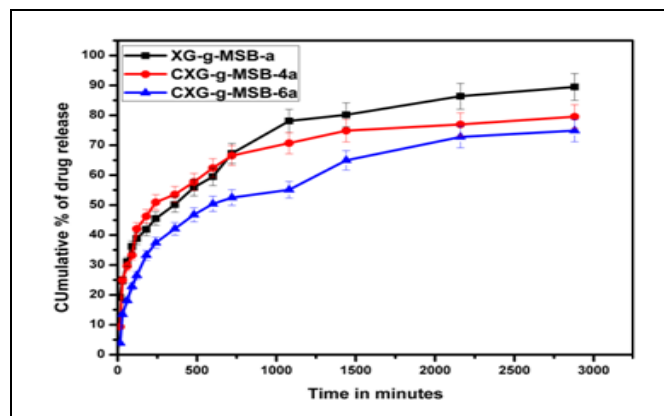


FIG. 9: VARIATION OF CS PERCENTAGE IN PH 7.4 AT 37 °C

Drug Release Kinetic Models:

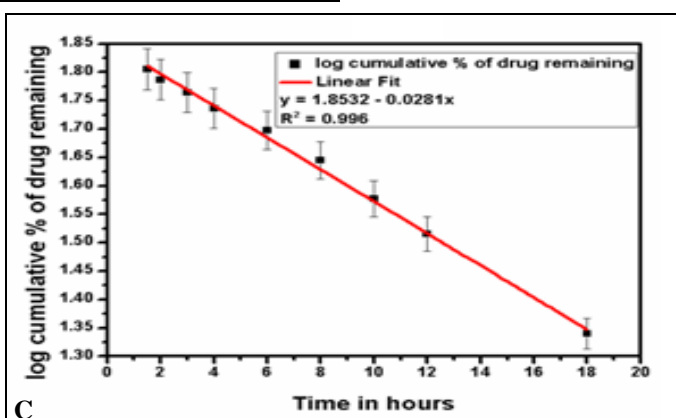
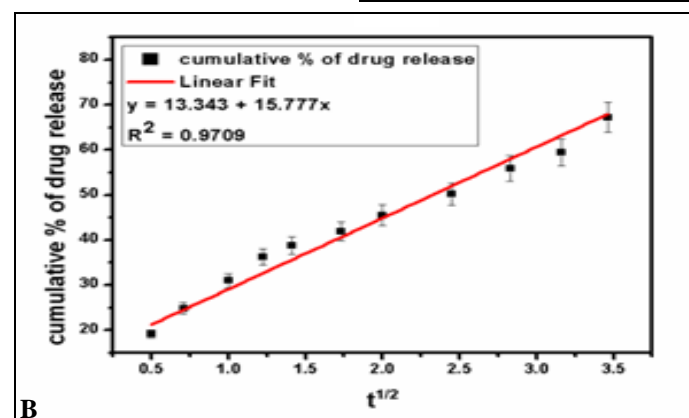
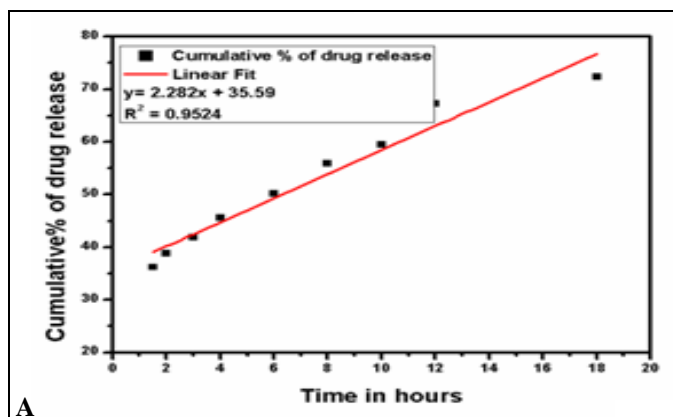


FIG. 10: ESTIMATION OF DRUG RELEASE MODEL: (A) ZERO TH ORDER (B) FIRST-ORDER AND (C) HIGUCHI MODEL

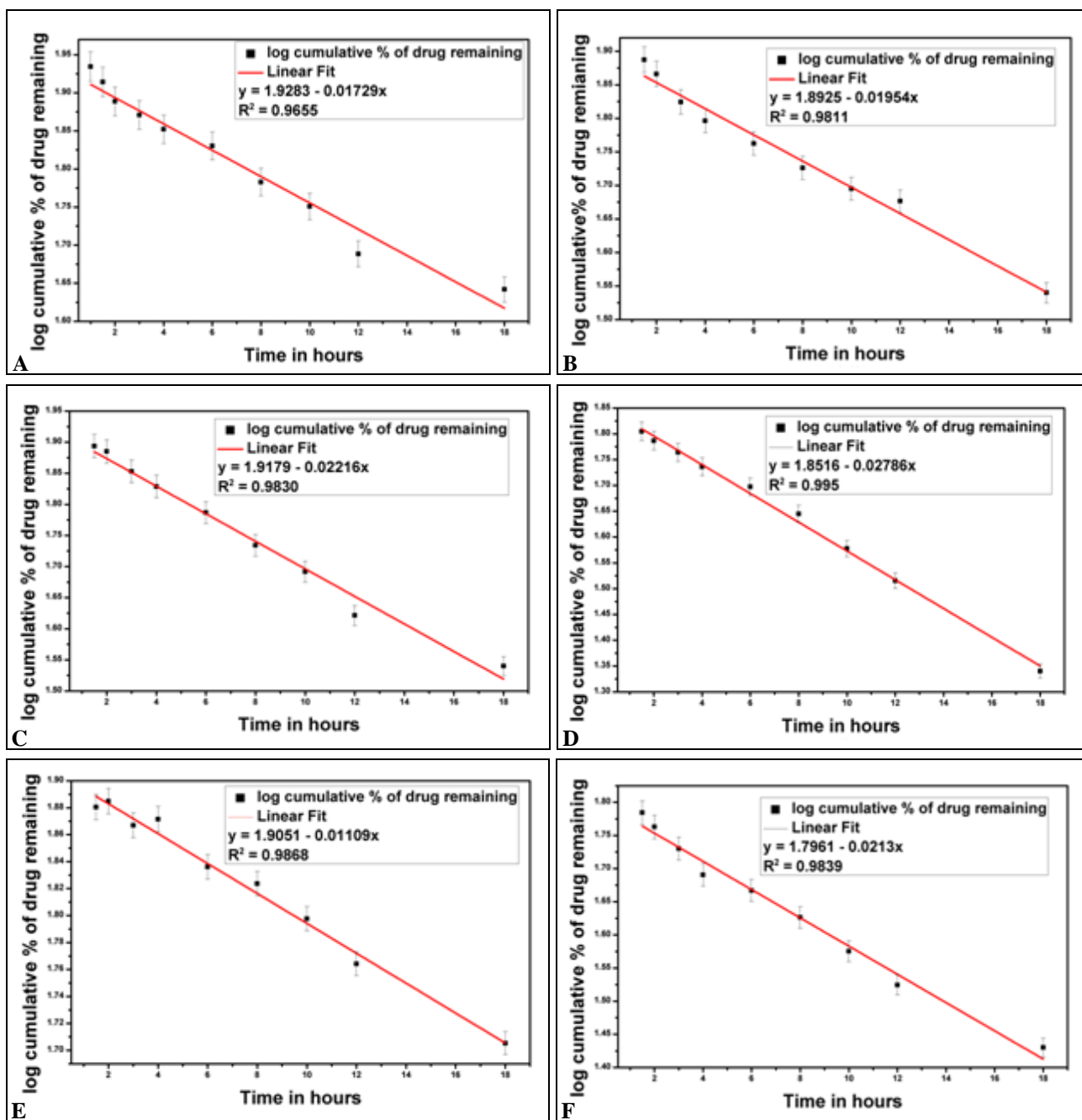


FIG. 11: FIRST ORDER ESTIMATION OF DRUG RELEASE. PLOTS OF LOG CUMULATIVE % OF DRUG REMAINING VERSUS TIME FOR DIFFERENT CONCENTRATIONS OF CT IN THE MICROSPHERES: XG-g-MSB-a (A), XG-g-MSB-b (B), CXG-g-MSB-4a (C), CXG-g-MSB-4b (D), CXG-g-MSB-6a (E) AND CXG-g-MSB-6b (F)

TABLE 3: MINIMUM DRUG CONTENT AFTER RELEASE (CO) AND HALF-LIFE OF ALL SAMPLES

S. no.	Sample	Drug conc. mg/ml	Co (mg/ml)	t _{1/2} (hrs)	r ²
1	XG-g-MSB-a	40	3.15	12.19	0.812
2	XG-g-MSB-b	30	2.71	21.95	0.831
3	CXG-g-MSB-4a	40	3.57	15.26	0.926
4	CXG-g-MSB-4b	30	4.68	28.73	0.977
5	CXG-g-MSB-6a	40	2.71	28.97	0.972
6	CXG-g-MSB-6b	30	5.01	25.47	0.951

The drug release kinetics of CT of all profiles was determined based on the best fit of kinetic models tested, which include: zeroth-order, first order, and Higuchi model. The correlation coefficient values

for zeroth-order, first order and Higuchi model are 0.952, 0.970 and 0.996 respectively **Fig. 10**. The correlation coefficient values were close to first order; therefore drug release kinetics of microbeads

follows first-order kinetics. For this reason, the first-order model was used to analyze the drug

release kinetics for all profiles, as shown in **Fig. 11**.

TABLE 4: DRUG RELEASE RATE CONSTANT AND CORRELATION COEFFICIENT OF ALL FORMULATIONS AFTER FITTING DRUG RELEASE DATA INTO DIFFERENT MATHEMATICAL MODELS

S. no.	Sample	Zero order		First order		Higuchi		Korsmeyer-Peppas	
		k ₀	r ²	k ₁	r ²	K _H	r ²	n	r ²
1	XG-g-MSB-a	12.4	0.951	1.95	0.965	14.4	0.978	0.428	0.961
2	XG-g-MSB-b	20.8	0.902	1.89	0.981	14.3	0.915	0.424	0.965
3	CXG-g-MSB-4a	16.6	0.880	1.93	0.983	14.6	0.884	0.369	0.996
4	CXG-g-MSB-4b	29.7	0.952	1.85	0.996	15.5	0.970	0.315	0.984
5	CXG-g-MSB-6a	18.3	0.901	1.90	0.986	10.0	0.966	0.322	0.983
6	CXG-g-MSB-6b	30.9	0.862	1.84	0.983	12.2	0.911	0.386	0.965

According to first-order kinetics, the drug release process is directly proportional to drug content involved in the process. Therefore the rate of the process increases linearly as the concentration of drug increases. In the present work, the duration of drug release shows 48-72 h; this reveals that the drug release kinetics of CT micro beads follows first-order kinetics. The minimum drug contents obtained after release (C₀) was calculated by using the following equation:

$$\ln C = \ln C_0 - kt \dots \dots \dots (13)$$

Where lnC₀ is the intercept, k is the slope and t corresponds to time. Similarly half-lives were determined using the following equation:

$$t_{1/2} = \ln 2/k \dots \dots \dots (14)$$

The results of the data fit to the first order and are given in **Table 4**. The data clearly shows that as the polymer-drug ratio increases, the elution rate also increases. The sample XG-g-MSB-a releases 89.4 % drug, leaving 10.6% whereas XG-g-MSB-b releases 62.6% drug, leaving 37.4%. Therefore higher the drug-polymer ratio, the higher the swelling rate, the faster the drug elution rate from the gel beads, as reported by previous researchers ³⁶.

The half-life (the time required for the concentration or amount of drug to be reduced by one-half) of CXG-g-MSB-6b See **Table. 3** showed the highest half-life 25.4 h, whereas XG-g-MSB-a showed the lowest half-life 12.1 h. The results confirm that the higher the drug-polymer ratio, the larger is the pore size, therefore faster is the elution rate. The drug release mechanism was further determined by plotting ln (Mt/M_∞) versus ln t (Korsmeyer-Peppas model). The n values obtained

for various formulations are presented in **Table 4**. The results are consistent with Fickian transport. Hence, the gel beads follow Fickian type diffusion.

CONCLUSION: In the present study, semi-IPN microbeads were fabricated from SA and modified XG. The grafting reaction was confirmed by FTIR. XRD and DSC confirmed the molecular level dispersion of drug in the polymer matrix. SEM and EDS studies revealed that the CS gel shell was successfully coated on the surface of microbeads. CS gel shell coated on the microbeads could increase the encapsulation efficiency. The *in-vitro* release study reveals that CS coated microbeads show a controlled release of CT. The controlled release characteristics of CT were dependent on blend ratio and % of CS coating. The *in-vitro* release results were fitted to the Peppas equation and the data supported the Fickian diffusion mechanism. Therefore, the developed microbeads are a potentially good candidate for novel drug delivery systems

ACKNOWLEDGEMENT: The authors M.C.S. Subha, K. Chowdoji Rao, and C. Madhavi thank the UGC for the financial support in the form of BSR fellowship.

CONFLICTS OF INTEREST: The authors have indicated that they have no conflicts of interest regarding the content of this article.

REFERENCES:

1. Ahmed EM, Aggor FS, Awad AM and El-Aref AT: An innovative method for preparation of nanometal hydroxide superabsorbent hydrogel. Carbohydrate Polymers 2013; 91: 693-98.
2. Brudno Y and Mooney DJ: On-demand drug delivery from local depots. Journal of Controlled Release 2015; 219: 8-17.

3. Li JL, Bai RB and Chen BH: Preconcentration of phenanthrene from aqueous solution by a slightly hydrophobic nonionic surfactant. *Langmuir* 2004; 20(14): 6068-70.
4. Mawad D, Stewart E, Officier DL, Romeo T, Wagner P, Wagner K and Wallace GG: A single component conducting polymer hydrogel as a scaffold for tissue engineering. *Advanced Functional Materials* 2012; 22: 2692-99.
5. Schmaljohann D: Thermo- and pH-responsive polymers in drug delivery. *Advanced Drug Delivery Reviews* 2006; 58: 1655-70.
6. Douglas A, Hall R, Horn DB, Kerr DNS, Pearson DT and Richardson H: Diuretic response to chlorthalidone. *British Medical Journal* 1961; 2(5246): 206-10.
7. Singer JM, O'Hare MJ, Rehm CR and Zarembo JE: Chlorthalidone. *Analytical Profiles of Drug Substances* 1985; 14: 1-36.
8. Talukdar M and Kinget R: Swelling and drug release behaviour of xanthan gum matrix tablets. *International Journal of Pharmaceutics* 1995; 120: 63-72.
9. Shalviri A, Liu Q, Abdekhodaie MJ and Wu XY: Novel modified starch-xanthan gum hydrogels for controlled drug delivery: synthesis and characterization. *Carbohydrate Polymers* 2010; 79: 898-07.
10. Gils PS, Ray D and Sahoo PK: Characteristics of xanthan gum-based biodegradable superporous hydrogel. *International Journal of Biological Macromolecules* 2009; 45: 364-71.
11. Andreopoulos AG and Tarantili PA: Xanthan Gum as a Carrier for Controlled Release of Drugs. *Journal of Biomaterials Applications* 2001; 16(1): 34-46.
12. Reddy OS, Subha MCS, JithendraT, Madhavi C, Rao KC and Mallikarjuna B: Sodium alginate/gelatin microbeads-intercalated with kaolin nanoclay for emerging drug delivery in Wilson's disease. *International Journal of Applied Pharmaceutics*, 2019; 11(5): 71-80.
13. Giri TK, Thakur D, Alexander A, Ajazuddin, Badwaik H and Tripathi DK: Alginate based hydrogel as a potential biopolymeric carrier for drug delivery and cell delivery systems: present status and applications. *Current Drug Delivery* 2012; 9: 539-55.
14. Cong Z, Shi Y, Wang Y, Wang Y, Niu J, Chen N and Xue H: A novel controlled drug delivery system based on alginate hydrogel/ chitosan micelle composites. *International Journal of Biological Macromolecules* 2018; 107:855-864.
15. Hutchens SA, Benson RS, Evans BR, O'Neill HM and Rawn CJ: Biomimetic synthesis of calcium-deficient hydroxyapatite in a natural hydrogel. *Biomaterials* 2006; 27: 4661-70.
16. Weng L, Gouldstone A, Wu Y and Chen W: Mechanically strong double network photocrosslinked hydrogels from N, N-dimethylacrylamide and glycidyl methacrylated hyaluronan. *Biomaterials* 2008; 29: 2153-63.
17. Kalia S: *Polymeric Hydrogels as Smart Biomaterials*. Springer International Publishing, First Edition 2016.
18. Sun X, Shi J, Xu X and Cao S: Chitosan coated alginate / poly (N-isopropylacrylamide) beads for dual responsive drug delivery. *International Journal of Biological Macromolecules* 2013; 59: 273-81.
19. Talukdar MM, Michoel A, Rombaut P and Kinget R: Comparative study on xanthan gum and hydroxyl-propylmethyl cellulose as matrices for controlled-release drug delivery I. Compaction and *in-vitro* drug release behaviour. *International Journal of Pharmaceutics* 1996; 129: 233-41.
20. Talukdar MM, Vinckier I, Moldenaers P and Kinget R: Rheological characterization of xanthan gum and hydroxypropylmethyl cellulose with respect to controlled-release drug delivery. *Journal of Pharmaceutical Sciences* 1996; 85(5): 537-40.
21. Kar R, Mohapatra S, Bhanja S, Das D and Barik B: Formulation and *in-vitro* characterization of xanthan gum-based sustained release matrix tablets of Isosorbide-5-Mononitrate. *Iranian Journal of Pharmaceutical Research* 2010; 9(1): 13-19.
22. Tao Y, Zhang R, Xu W, Bai Z, Zhou Y, Zhao S, Xu Y and Yu D: Rheological behavior and microstructure of release-controlled hydrogels based on xanthan gum crosslinked with sodium trimetaphosphate. *Food Hydrocolloids* 2016; 52: 923-33.
23. Martínez-Gómez F, Guerrero J, Matsuhiro B and Pavez J: *In-vitro* release of metformin hydrochloride from sodiumalginate / polyvinyl alcohol hydrogels. *Carbohydrate Polymers* 2017; 155: 182-91.
24. Fareez IM, Lim SM, Mishra RK and Ramasamy K: Chitosan coated alginate-xanthan gum bead enhanced pH and thermotolerance of *Lactobacillus plantarum* LAB12. *International Journal of Biological Macromolecules* 2015; 72: 1419-28.
25. Pongjanyakul T and Puttipipatkachorn S: Xanthan-alginate composite gel beads: Molecular interaction and *in-vitro* characterization. *International Journal of Pharmaceutics* 2007; 331: 61-71.
26. Pandey S and Mishra SB: Graft copolymerization of ethylacrylate onto xanthan gum, using potassium peroxydisulfate as an initiator. *International Journal of Biological Macromolecules* 2011; 49: 527-35.
27. Zhenga M, Lian F, Zhu Y, Zhang Y, Liu B, Zhang L and Zheng B: pH-responsive poly (xanthan gum-g-acrylamide-g-acrylic acid) hydrogel: Preparation, characterization, and application. *Carbohydrate Polymers* 2019; 210: 38-46.
28. Pandey PK, Banerjee J, Taunk K and Behari K: Graft copolymerization of acrylic acid onto xanthan gum using a potassium monopersulfate/Fe²⁺ redox pair. *Journal of Applied Polymer Science* 2003; 89: 1341-46.
29. Kumar A, Deepak, Sharma S, Srivastava A and Kumar R: Synthesis of xanthan gum graft copolymer and its application for controlled release of highly water soluble Levofloxacin drug in aqueous medium. *Carbohydrate Polymers* 2017; 171: 211-19.
30. Gupta KC and Sahoo S: Grafting of N, N'-methylenebisacrylamide onto cellulose using Co (III)-acetylacetonate complex in aqueous medium. *Journal of Applied Polymer Science* 2000; 76: 906-12.
31. Gupta KC and Gupta SK: Grafting of N,N'-Methylenebisacrylamide onto silk fibers using the vanadylacetylacetonate complex in aqueous medium. *Journal of Applied Polymer Science* 1987; 33:2849-2857.
32. Madhavi C, Babu PK, Maruthi Y, Parandhama A, Reddy OS, Rao KC, Subha MCS and Kumar RJ: Sodium alginate-locust bean gum IPN hydrogel beads for the controlled delivery of nimesulide-anti-inflammatory drug. *International Journal of Pharmacy and Pharmaceutical Sciences* 2017; 9: 245-52.
33. Dash S, Murthy PN, Nath L and Chowdhury P: Kinetic modeling on drug release from controlled drug delivery systems. *Acta Poloniae Pharmaceutica-Drug Research* 2010; 67(3): 217-23.
34. Gouda R, Baishya H and Qing Z: Application of mathematical models in drug release kinetics of Carbidopa and Levodopa ER tablets. *Journal of Developing Drugs* 2017; 6: 2-8.

35. Dozie-Nwachukwu SO, Danyuo Y, Obayemi JD, Odusanya OS, Malatesta K and Soboyejo WO: Extraction and encapsulation of prodigiosin in chitosan microspheres for targeted drug delivery. *Materials Science and Engineering* 2017; 71: 268-78.
36. Costa P and Lobo JMS: Modeling and comparison of dissolution profiles. *European Journal of Pharmaceutical Sciences* 2001; 13: 123-33.
37. Prasad CV, Swamy BY, Mallikarjuna B, Sreekanth KC, Subha MCS, Rao KC and Yu J: Preparation and characterization of interpenetrating polymer network beads for controlled release of acebutolol hydrochloride. *Advances in Polymer Technology* 2012; 31(2): 87-99.
38. Elella MHA, Mohamed RR, ElHafeez EA and Sabaa MW: Synthesis of novel biodegradable antibacterial grafted xanthan gum. *Carbohydrate Polymers* 2017; 173: 305-11.
39. Eswaramma S, Reddy NS and Rao KSVK: Carbohydrate polymer based pH-sensitive IPN microgels: Synthesis, characterization and drug release characteristics. *Materials Chemistry and Physics* 2017; 195: 176-86.
40. Reddy OS, Subha MCS, Jithendra T, Madhavi C and Rao KC: Emerging novel drug delivery system for control release of curcumin through sodium alginate / poly (ethylene glycol) semi IPN microbeads-intercalated with kaolin nanoclay. *Journal of Drug Delivery and Therapeutics* 2019; 9(3-s): 324-33.
41. Eswaramma S and Rao KSVK: Synthesis of dual responsive carbohydrate polymer based IPN microbeads for controlled release of anti-HIV drug. *Carbohydrate Polymers* 2017; 156: 125-34.

How to cite this article:

Jithendra T, Reddy OS, Subha MCS, Madhavi C and Rao KC: Xanthan gum graft copolymer/sodium alginate micro beads coated with chitosan for controlled release of chlorthalidone drug. *Int J Pharm Sci & Res* 2020; 11(3): 1132-45. doi: 10.13040/IJPSR.0975-8232.11(3).1132-45.

All © 2013 are reserved by the International Journal of Pharmaceutical Sciences and Research. This Journal licensed under a Creative Commons Attribution-NonCommercial-ShareAlike 3.0 Unported License.

This article can be downloaded to **Android OS** based mobile. Scan QR Code using Code/Bar Scanner from your mobile. (Scanners are available on Google Playstore)